Evolution, 51(5), 1997, pp. 1561–1573

THE *PONTIA DAPLIDICE-EDUSA* HYBRID ZONE IN NORTHWESTERN ITALY

ADAM H. PORTER,[1,2,3] REMO WENGER,[4] HANSJÜRG GEIGER,[4] ADOLF SCHOLL,[4] AND ARTHUR M. SHAPIRO[5]
[1]*Department of Biological Sciences, Bowling Green State University, Bowling Green, Ohio 43403–0212*
[2]*E-mail: aporter@ent.umass.edu*
[4]*Zoologisches Institut der Universität Bern, Baltzerstrasse 3, CH-3012 Bern, Switzerland*
[5]*Section of Evolution and Ecology, University of California, Davis, California 95616*

Abstract.—The pierid butterflies *Pontia daplidice* and *P. edusa*, parapatrically distributed in southern Europe, have very similar morphologies and life histories, but show fixed differences at four allozyme markers. We sampled these allozymes in a 28-population transect north of Genoa in Italy, through the hybrid zone where these taxa meet. We used the numerical techniques developed for hybrid zone analysis to study the patterns of genetic differentiation and their underlying evolutionary causes. The hybrid zone is characterized by a very short and steep central region, flanked by broad tails of introgression extended up to 100 km in either direction. From mean two-locus disequilibium of $D = 0.148$ (maximum-likelihood two-unit support limits 0.139–0.153), and after accounting for minor differences in the center locations of the single-locus clines, which act to bias the dispersal estimate, we estimated a dispersal rate of $\sigma = 4.4$ (3.7–5.5) km/gen$^{1/2}$. The effective selection needed to maintain the steep central portion is strong, $0.47 \leq s^* \leq 0.64$, when combined over potential intrinsic (genetic background) and extrinsic (ecological) sources of selection. The clines in allozyme loci showed variation that was significantly different between the most divergent shapes, and the differences are attributable to different degrees of introgression on the *edusa* side of the zone. The average selection acting on individual allozyme loci was high at $s_e \approx 1.5\%$, but because of the narrowness of the central region of the cline, we suspect that this estimate is somewhat biased by selection on loci closely linked to the allozyme markers. A common question for taxa that show fixed allozyme differences in parapatry is whether or not they are genetically isolated. A fairly general measure of genetic isolation across hybrid zones is the time, T, that it takes a neutral allele to cross the hybrid zone and recombine into the opposite genetic background, given by $T = (\beta/\sigma)^2$, where β is the barrier strength of the hybrid zone. Genetic isolation in the *Pontia* zone is weak, with $T \approx 25$ generations for most allozyme markers. By this measure, populations of *daplidice* and *edusa* on opposite sides of the hybrid zone share more identical-by-descent alleles than do populations of phenotypically pure *daplidice* in, say, France and Morocco. Accordingly, we think it best for systematists to consider *edusa* as a well-marked subspecies of *P. daplidice*.

Key words.—Allozyme, butterfly, cline, dispersal, genetic isolation, genetic population structure, introgression, Lepidoptera, Pieridae, *Pieris*, selection.

Received December 9, 1996. Accepted May 21, 1997.

Among the long-standing problems of evolutionary biology is the need to provide explanations for patterns of geographic diversity in the traits of closely related organisms. Traditionally, systematists have described these patterns, and one particularly common assumption in species-level systematics, implicit in any attempt to organize populations into species or infraspecific categories, is that the "diagnostic" traits are markers for more fundamental genomic differentiation. For species under the isolation concept (Coyne et al. 1988), diagnostic traits indicate genetic isolation. In fact, this does not necessarily hold for sexually reproducing organisms, as selection may maintain differences in diagnostic traits even while permitting substantial gene exchange at other loci (Barton and Bengtsson 1986). Even genetic drift under an isolation-by-distance model of population structure leads to patterns of geographic differentiation in neutral traits that may persist for hundreds of generations (Endler 1977), and such traits could be taken erroneously as taxonomically diagnostic in many cases. Nevertheless, as the existence of sibling species emphasizes, even subtle diagnostic traits may sometimes represent more fundamental genomic differentiation, and indicate genetic isolation among the sets of populations. A continuum of degrees of genetic isolation may exist between population groups, and taxonomic decisions based on diagnostic traits should not, as they often are, be treated as firm conclusions. Species-level taxonomic alternatives represent competing hypotheses about underlying genetic structure that depend on the correlations between putatively diagnostic markers and the remainder of the genome. Testing these hypotheses is an empirical problem in the genetic structuring of populations, and it may be addressed using the methods of population biology (Porter and Geiger 1988; Otte and Endler 1989; Porter 1990).

Porter and Geiger (1995) used hierarchical F-statistics (Weir and Cockerham 1984; Slatkin 1987; Porter 1990; Cockerham and Weir 1993), isolation-by-distance (Slatkin 1993), and spatial autocorrelation (Sokal and Oden 1978) methods to investigate the ability of taxonomically diagnostic traits to predict more widespread genetic differentiation among taxa within the *Pieris napi* species group (Lepidoptera: Pieridae) throughout Europe. They found no evidence in allozyme data of any meaningful genetic differentiation between the currently recognized taxa, but they pointed out that all these analyses relied upon a critical untested assumption that the populations have approached equilibrium patterns of genetic differentiation. The broad geographic ranges of subspecies or parapatric species in most organisms implies that their total populations have tremendously large effective sizes. This means, first, that if these taxa have indeed become genetically isolated, they will be drifting apart so slowly that only negligible differentiation is likely to have accumulated

[3] Present address: Department of Entomology, University of Massachusetts, Amherst, Massachusetts 01003.

in neutral markers. Second, such small drift rates are easily overcome by selection, even for many loci that are "nearly neutral" at smaller spatial scales. Regional-scale averages of enzyme allele frequencies may thus reflect unknown contributions from either a lack of time since genetic isolation, similar selective histories, or both, in addition to the presumed contributions from the present rate of gene exchange. The limitations of assuming equilibrium over broad spatial scales may be overcome by studying selection and gene flow in hybrid zones, or, if no hybridization occurs, in contact areas. There, local spatial scales are relevant and the associated effective population sizes are much smaller, and evolutionary rates considerably faster. Equilibrium genetic structures on this scale are likely to be approached to within the range of sampling error within a few thousands of generations or less (Crow and Aoki 1984). Patterns on these local scales are more likely to reflect present-day evolutionary processes.

Powerful methods are available to study evolution in hybrid zones (Harrison 1993). Most animal hybrid zones may be modeled as equilibria between selection, which enforces differentiation on either side, and gene exchange, which leads to the mixing of the genomes on either side (Slatkin 1973; Endler 1977; Barton and Hewitt 1985; Barton and Gale 1993). Such zones provide barriers even to neutral alleles, which experience selection via their inevitable correlations in hybrids to loci under selection (Barton and Hewitt 1983; Barton and Bengtsson 1986). The barriers are typically not absolute because these disequilibria decay with recombination, and alleles escape into favorable genetic backgrounds on the other side of the zone. However, the barriers may be quite strong if there are enough selected loci that all neutral loci are likely to experience close linkage to one or more of them (Barton and Bengtsson 1986). Moreover, these barriers are expected to vary among loci in the same hybrid zone because of variance among loci in their linkage to selected traits.

By fitting models of cline shape to allozyme marker data using numerical techniques (Szymura and Barton 1986, 1991; Mallet et al. 1990; Barton and Gale 1993), one may obtain estimates of the values of a wide variety of evolutionarily relevant parameters. In addition to dispersal and selection estimates, one may compute a barrier strength, β, in units of geographic distance (Barton and Bengtsson 1986; Szymura and Barton 1986, 1991). Populations on opposite sides of a hybrid zone can be considered as sharing the same proportion of neutral alleles as would taxonomically "pure" populations separated from one another by distance β in a standard isolation-by-distance model. This barrier may differ from species to species simply because of differences in dispersal rates, but we can standardize the parameter to a per-generation time scale $T = (\beta/\sigma)^2$ using the dispersal rate σ, in a manner analogous to the computation of a coefficient of variation. T, the time needed to travel across the hybrid zone (Barton and Gale 1993), can then be used as a standard measure of the degree of genetic isolation across hybrid zones. If T is large enough, say 10^6 generations, then we can say the taxa are genetically isolated; 10^6 generations is arbitrarily chosen, but this value is roughly the reciprocal of the mutation rate, and alleles identical in state would be expected to arise anyway on the opposite side of the zone within this time span.

In this paper, we investigate the degree of genetic isolation between two genetically distinct but morphologically very similar taxa within the nominal butterfly species *Pontia daplidice* L. (Pieridae) in the Mediterranean basin (Geiger and Scholl 1985; Geiger et al. 1988). These taxa are parapatric with strong genetic differences, which is a relatively common biogeographic pattern among animal species groups. The taxonomy is unresolved, and in this paper we drop the genus name to emphasize this uncertainty. The taxon *daplidice* (L.) (sensu Wagener 1988) is distributed from France to Morocco, and also occurs in Israel and southeastern Turkey. The other taxon, *edusa* (F.) (sensu Wagener 1988), is found from Italy and Corsica through the Balkans and Greece to central Turkey, and taxonomically unresolved populations of the *daplidice* group occur across to the cold steppe habitats of south-central Russia. In the mediterranean basin, *daplidice* and *edusa* differ in allele substitutions at four of 17 allozyme loci surveyed. At the loci GOT-1, GPT, GPDH and 6-PGD, the two taxa only very rarely show alleles in common. Modest laboratory studies suggested some postmating barriers in crosses between specimens from France and Greece, with one of four crosses yielding viable offspring and the remainder showing only partial embryonic development (Geiger et al. 1988), though a second study found no differences in F_1, F_2, and backcross survivorship, fecundity, or development (Büchi 1996). Both *daplidice* and *edusa* are common butterflies, with high dispersal and frequent population turnover characteristic of organisms sharing their early successional habitats (Courtney and Chew 1987), and lepidopterists were surprised to find such striking geographic variation in their allozymes. Sympatric species of pierids often show less differentiation, and the question of the degree of genetic isolation between them is a natural one, both here and in many such groups of organisms. Based on the locations of genetically diagnosed populations studied by Geiger et al. (1988), we searched for a hybrid zone in northwestern Italy in which to investigate the local-scale patterns of genetic structure, and more usefully, their underlying causes and the expected evolutionary consequences.

Materials and Methods

In 1990 and 1991, 483 specimens distributed among 28 sampling sites (Table 1) were collected along a transect running 167 km in length in Italy north of Genoa (Fig. 1). The suitable habitat is distributed in a broad band oriented approximately west to east in the sampled region. We therefore oriented our transect line west to east (Fig. 1), and the distance along this line from the western-most end was taken as the geographic location of each site (Table 1).

Butterflies were frozen in liquid nitrogen immediately upon collection in the field and stored in the laboratory at -80°C until electrophoretic analysis. Vertical starch gel electrophoresis of allozymes was conducted using routine techniques (Geiger 1981; Geiger and Scholl 1985). The same 17 enzyme loci as investigated in Geiger et al. (1988) were scored, yielding comparable within-population patterns of genetic diversity as found in that study; these results are reported in Wenger (1993). Of these 17 loci, the loci GOT-1, GPT, GPDH, and 6-PGD, which are fixed for different marker alleles in

TABLE 1. Names, sizes, and locations of sample sites along the transect.

No.	Site	*n*	Location (km)
1	Diano	6	0.0
2	Alba	9	0.6
3	Camerana	10	6.2
4	Gorzegno	5	7.0
5	Castino	33	10.4
6	Roccaverano	15	17.6
7	Vengore	13	21.6
8	Monastero	9	23.2
9	Bistagno	19	26.0
10	Pareto	58	26.2
11	Molare	8	42.6
12	Alice	13	60.4
13	Voltaggio	42	64.2
14	Rocchetta	11	80.2
15	Godiasco	30	81.6
16	Bagnaria	21	87.2
17	Fabbrica	27	89.0
18	Varzi	27	91.6
19	Bobbio	11	107.2
20	Fabbiano	7	123.6
21	Bettola	6	124.8
22	Cassano	17	126.4
23	Gazzo	7	133.8
24	Varsi	11	144.0
25	Serravalle	19	152.0
26	Varano	17	156.3
27	Viazzano	12	160.8
28	Medesano	17	167.0

daplidice and *edusa*, were used for the hybrid zone analyses below. 6-PGD is sex-linked and the others are autosomal (Büchi 1996), and this was accounted for in our analyses.

Analysis

Hybrid zones are concordant clines in different characters (Barton and Hewitt 1985), and selection acting on different characters combines synergistically to make the hybrid zone steeper than each of the clines would be if they existed alone (Barton 1983; Baird 1995). The shape of a multilocus cline (Barton 1983) is approximated most easily by combining three single-locus equations (Szymura and Barton 1986, 1991),

$$p = \exp\left[\frac{4(x - [c + z_L])\sqrt{\theta_L}}{w}\right], \quad (1a)$$

$$p = \frac{1}{2}\left[1 + \tanh\left(\frac{2[x - c]}{w}\right)\right], \quad (1b)$$

$$p = 1 - \exp\left[\frac{-4(x - [c - z_R])\sqrt{\theta_R}}{w}\right], \quad (1c)$$

where equation (1b) is a sinusoidal shape in the center, and equations (1a) and (1c) are (potentially different) exponential decays on either side leading away from this center (Fig. 2). The parameter definitions are summarized in Table 2. These equations are related in that as θ and z approach one and zero, respectively, equations (1a) and (1c) approach the shape of equation (1b) on their respective sides of the zone. These equations together contain six potentially independent parameters describing the shape of the hybrid zone, and estimating the values of these parameters from data requires

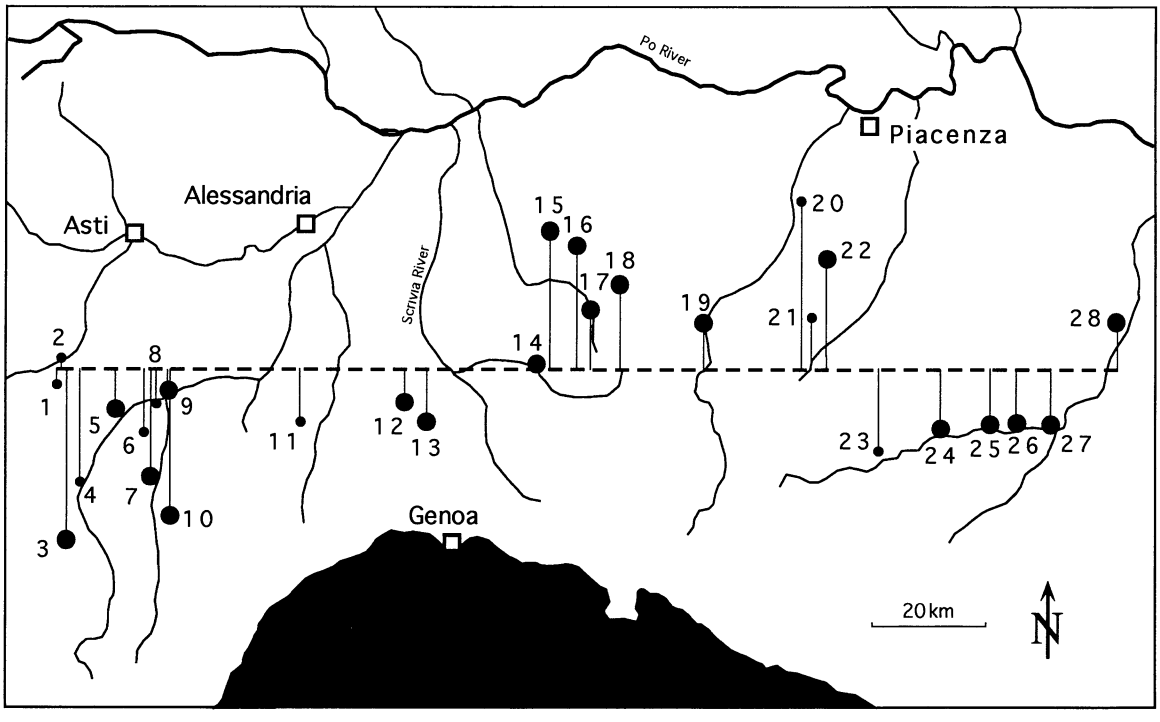

FIG. 1. Geographical location of samples and the course of the transect line in northwestern Italy. Population numbers correspond to those in Table 1. Small points: $n < 10$; large points: $n \geq 10$.

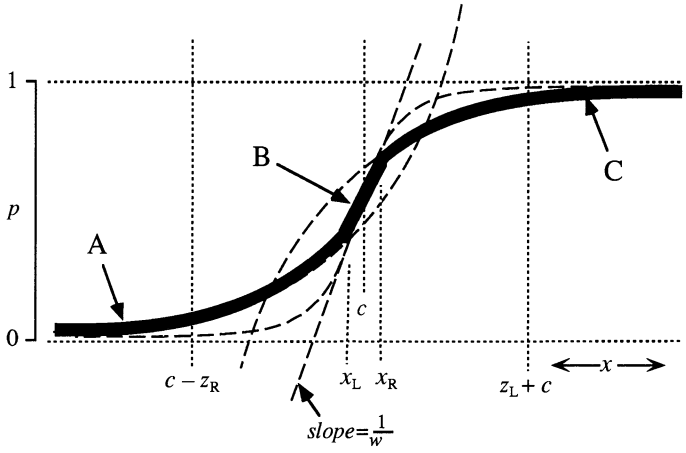

FIG. 2. Hybrid zone shape is estimated from models by cobbling together the equations *A*, *B*, and *C*, given in the text (eqs. 1a,b,c) and in Szymura and Barton (1986, 1991). The parameters are defined in Table 2.

numerical techniques. In addition, gametic disequilibrium (D) in the hybrid zone can provide information about the strength of selection in the center of the zone (Szymura and Barton 1986, 1991; Barton and Gale 1993). The value of this approach to cline description is that equations (1a,b,c) are derived from first principles using the fundamental evolutionary parameters of gene flow and selection. Once data have been fit to these equations, these fundamental parameters may also be estimated, yielding considerable insight into underlying evolutionary processes in and around the hybrid zone.

Following Szymura and Barton (1986, 1991), we used maximum likelihood (see Edwards 1992) to fit the data to the hybrid zone model. Under this approach, the seven parameters (six shape parameters and D) can be varied continuously and independently, and each potential set of values can be seen as a separate hypothesis about the shape of the cline. Again following Szymura and Barton (1986, 1991), the fitting to the likelihood model was done numerically by writing a Metropolis (= simulated annealing) algorithm (Press et al. 1989). Values of each of the seven parameters were randomly varied following Gaussian distributions with zero means and arbitrary variances, and the log-likelihood (L) recalculated for each iteration. The set of parameter estimates were "accepted" as initiating points of the subsequent iteration if the new L' was higher. If L' was lower, the set was only accepted with a probability of $\exp(L/L')$, which represents the ratio of the two likelihoods. This process creates a bounded random walk that settles around the maximum-likelihood estimate (L_{max}), and tends to walk out of any locally maximal likelihoods and find the global maximum (Press et al. 1989). The "annealing" process is achieved by gradually narrowing the variances of the random walk by degrees between each round of iterations. Support limits of $L_{max} - 2$ were used to obtain confidence intervals analogous to 95% confidence limits, as recommended by Edwards (1992). These limits were obtained after the initial annealing process by running the random walk at sampling variances that yield approximately $\exp(L_{max}/L') = 0.5$. This criterion simply gives the most efficient algorithm and the actual values of these variances do not affect the support-limit estimation as long as a sufficient proportion of replicates falls below $L_{max} - 2$. A program for these calculations, in Think® Pascal (vers. 4.2, Macintosh), is available from A. Porter.

The best fitting model maximizes the statistic $L = L(S) + L(D, S) + C$, where $L(S)$ is the log-likelihood of the estimates yielding hybrid zone shape, and $L(D, S)$ is the log-likelihood of the disequilibrium estimate in the central region of the cline. C is an arbitrary constant of proportionality common to all likelihood models (Edwards 1992), and is hereafter dropped from the notation. L is proportional to the log of a probability (Edwards 1992), thus $L \leq 0$. For cline shape estimated from frequency data, the log-likelihood of the model given the data derives from the binomial distribution following the logic of the contingency-table statistic G (Sokal and Rohlf 1995, p. 686). It is

TABLE 2. Definitions of paramters used.

β_L	Barrier to gene flow from the *daplidice* (left) to the *edusa* (right) side of the zone, in units of distance
β_R	Barrier to gene flow from the *edusa* to the *daplidice* side of the zone, in units of distance
c	Location of the center of the zone on the x-axis
D	Average 2-locus gametic disequilibrium
S	The vector of six parameter values that determine cline shape, $\{c, w, \theta_L, \theta_R, z_L, z_R\}$
σ	Dispersal per generation; the standard deviation of distances between birthplaces of parents and offspring
s^*_{ex}	Effective strength of selection against recombinant gentoypes due to inappropriate responses to environmental conditions (extrinsic selection)
s^*_{in}	Effective strength of selection against recombinant gentoypes due to inappropriate interactions among loci (intrinsic selection)
s_{eL}	Selection acting directly on each marker locus in the left tail of the zone
s_{eR}	Selection acting directly on each marker locus in the right tail of the zone
θ_L	The exponential decay of the left side of the zone relative to the shape of the central cline of eqn. (1b)
θ_R	The exponential decay of the right side of the zone relative to the shape of the central cline of eqn. (1b)
T_L	Time in generations for a neutral allele to diffuse from the *daplidice* (left) to the *edusa* (right) side of the zone
T_R	Time in generations for a neutral allele to diffuse from the *edusa* to the *daplidice* side of the zone
w	Width of the zone, equal to 1/slope at the center of the zone
x	(Geographic) location along the transect, in km units
x_L	Location of the intersection between cline shape eqns. (1a) and (1b)
x_R	Location of the intersection between cline shape eqns. (1b) and (1c)
z_L	Distance from c of a vertical asymptote for the exponential decay on the left side of the zone
z_R	Distance from c of a vertical asymptote for the exponential decay on the right side of the zone

$$L(S) = \sum_i \sum_j \left[\sum_k p_{ijk} \ln\left(\frac{p_{ijk}}{p[S, x_i]}\right) + \sum_k (1 - p_{ijk}) \ln\left(\frac{1 - p_{ijk}}{1 - p[S, x_i]}\right)\right], \quad (2)$$

where p_{ijk} is the allele frequency of the jth individual at the kth locus in the ith population sample, and $p(S, x_i)$ is the expected frequency of the *edusa* allele predicted from the model at sampling location x_i with shape parameters $S = \{c, w, \theta_R, \theta_L, z_R, z_L\}$, as given by equations (1a,b,c) (see Table 2). The likelihood model differs from that in a standard heterogeneity analysis only in that the expected values of gene frequencies $p(S, x_i)$ are not everywhere constant, but vary with the location x along the cline. Numerically varying the values of shape parameters S then produces different expected values of cline shape, and the highest likelihood corresponds to the best-fitting set of shape parameters. Occasionally, randomly generated combinations of estimates in cline shape S yield equations (1a,b,c) that never intersect, a situation that would be biologically meaningless because S approximates a continuous cline, so these were rejected in the estimation procedure.

The log-likelihood of the disequilibrium estimate, $L(D, S)$, was calculated for all sample sites in the central region of the cline using a modified version of Hill's (1974) likelihood model (see Appendix). The formula is

$$L(D, S) = \sum L(D, S, x), \quad (3)$$

where $L(D, S, x)$ is the log-likelihood of D for the sample at location x on the cline. There is no standard method available for determining the extent of the central region when clines are steep, so after initial runs of the shape model alone, we arbitrarily chose the central region to be within 25 km of the center point c. The log-likelihood at location x is approximately the sum of log-likelihoods for each pairwise combination of the d diagnostic loci,

$$L(D, S, x) = \sum_{a=1}^{d-1} \sum_{b=a+1}^{d} L(D, S, x, a, b), \quad (4)$$

where $L(D, S, x, a, b)$ is the log-likelihood of D for a particular pairwise combination of loci (Appendix, eq. A2), and indices a and b represent those loci. Higher-order disequilibria were ignored, following Barton and Gale (1993). For each pairwise combination, diagnostic alleles were pooled for each side of the hybrid zone and the log-likelihood function (Hill 1974) is

$$L(D, S, x, a, b) = C + \sum_i^2 \sum_j^2 X_{ij} \ln f(D, S, x)_{ij} + N_{22} \ln[f(D, S, x)_{11} f(D, S, x)_{22} + f(D, S, x)_{12} f(D, S, x)_{21}], \quad (4b)$$

where matrices **N** and **X** are defined in the Appendix. $\boldsymbol{f}(\boldsymbol{D}, \boldsymbol{S}, \boldsymbol{x})$ is a matrix of expected genotype frequencies as defined for the matrix $\boldsymbol{f}$ in the Appendix, with the additional constraint that disequilibrium D_{adj} is adjusted for its position x along the cline predicted by the model of shape S. The adjustment is

$$D_{adj} = \frac{D(1 + F_{IS})}{p(S, x)[1 - p(S, x)]}, \quad (5)$$

because disequilibrium is constrained by the maximum allele frequency, which decays away from the center of the cline (Barton and Gale 1993). Following Nürnberger et al. (1995), the factor $(1 + F_{IS})$ adjusts for deviations from Hardy-Weinberg proportions, which act to confound disequilibrium estimation (Weir and Cockerham 1979; Barton and Gale 1993). F_{IS} was estimated for the central region using the sample-size adjusted formula of Weir and Cockerham (1984). Occasionally, values of $f(D, S, x)_{ij} \leq 0$ occur because of sampling variation, meaning that $L(D, S, x, a, b)$ is undefined for that locus pair. Such biologically meaningless values were reset to 10^{-10}, which yields a very low, but finite, likelihood, such that the algorithm rejected those values. The number of populations in the central region may vary with cline shape, and since $L(D, S)$ depends on the number of populations in the central region, support limits for D and parameter estimates dependent upon it (below) were obtained separately for each combination of central populations. In reporting these derived parameter estimates, the averages of the maximum-likelihood estimates over population combinations are given, and the support limits are taken over all population combinations. The Metropolis method is not limited by the presence of multiple peaks in $L(D, S)$, as is Hill's (1974) iterative maximum-likelihood solution (Weir and Cockerham 1979); thus, the alternative numerical methods recommended for finding the roots of $L(D, S)$ (Weir and Cockerham 1979) were not necessary.

From each set of parameter estimates (D and S), several other parameters relevant to biological processes in hybrid zones can be calculated. These derived parameters were estimated for each iteration, and support limits of $L_{max} - 2$ were obtained for each. Specifically, the rate of dispersal (σ, the standard deviation of distances between birthplaces of parents and offspring) can be estimated as

$$\sigma = \sqrt{\frac{Drw^2}{1 + r}}, \quad (6)$$

where D is the disequilibrium coefficient, w is the hybrid zone width, and r is the harmonic mean recombination rate among loci under selection (Szymura and Barton 1991; Barton and Gale 1993). The harmonic mean recombination rate was estimated numerically as

$$\frac{1}{r} = \frac{2(C - 1)}{C} + \frac{C}{R^2} \sum_{y=0}^{R/C} \ln\left(\frac{e^{2y} - 1}{2r_0}\right) \quad (7)$$

(Szymura and Barton 1991), where C is the effective number of chromosomes, R/C is the average chromosome length, and the summation is over steps of size $r_0 = 10^{-5}$. Lepidoptera generally have numerous small chromosomes of about equal size. *Pontia daplidice* and *P. edusa* both have $C = 26$ chromosomes, and this was taken as the effective chromosome number. This yields an estimate of $r = 0.385$. The estimate is slightly influenced by the size of r_0, which represents the minimum recombination distance between a neutral locus and a locus under selection, but in practice, there was no change in r when r_0 differed by a factor of 10.

The effective strength of selection against hybrid geno-

types (s^*) can be estimated from the width (σ) and the rate of dispersal (s), using the relationship

typo: should be = quantity squared

$$s^* = \sqrt{\frac{k\sigma}{w}}, \quad (8)$$

where k is a constant that depends on the general type of selection that drives the hybrid zone (Barton and Gale 1993). If the selection is "intrinsic" s^*_{in}, acting against heterozygous genotypes due to the genetic background, then $k = 2$. For "extrinsic" selection, s^*_{ex}, produced by genotypes favored on separate sides of an environmental gradient, then $k = 1.732$ (Barton and Gale 1993). Both estimates of s^* were calculated.

The effective selection (s_{eL}, s_{eR}) acting on each marker locus can be estimated from s^* and the decay rates (θ_L, θ_R; Fig. 2) on either side of the zone. The rationale is that away from the center of the zone, disequilibrium among selected loci drops to near zero and each introgressing locus evolves relatively independently (Barton 1983). The average effective selection on each marker locus is $s_{eL} = \theta_L s^*$ and $s_{eR} = \theta_R s^*$ (Szymura and Barton 1986, 1991). For these estimates, we used s^*_{in}.

Hybrid zones produce barriers to neutral genes because such genes are linked to genes experiencing selection (Barton 1979; Barton and Hewitt 1983; Barton and Bengtsson 1986). The barriers are potentially different for genes going different directions across the zone, and their strengths (β_L, β_R) can be estimated from the cline shape in the regions (x_L, x_R) where the exponential tails join the steeper central portion. Specifically, the strengths are

$$\beta_L = \frac{\Delta p}{\left(\frac{\partial A}{\partial x}\right)} \quad \text{evaluated at } x_L, \quad (9a)$$

$$\beta_R = \frac{\Delta p}{\left(\frac{\partial C}{\partial x}\right)} \quad \text{evaluated at } x_R, \quad (9b)$$

where A and C are equations (1a) and (1c) and Δp is the difference $p(S, x_R) - p(S, x_L)$. The derivatives are

$$\frac{\partial A}{\partial x} = \frac{4\sqrt{\theta_L}}{w}\exp\left[\frac{4(x - [c + z_L]\sqrt{\theta_L})}{w}\right], \quad (10a)$$

$$\frac{\partial C}{\partial x} = \frac{4\sqrt{\theta_R}}{w}\exp\left[\frac{4(x - [c + z_R]\sqrt{\theta_R})}{w}\right], \quad (10b)$$

and were obtained using Mathematica (Wolfram 1991). These barriers are in units of distance, and between any pair of locations, isolation-by-distance in continuously favorable environments can produce similar levels of genetic differentiation in neutral alleles, depending on dispersal rate and the distance separating the populations (Wright 1943; Slatkin 1993). The barriers are thus interpreted as the geographic distance separating populations in a continuous, homogeneous environment that would yield equivalent differentiation to that seen in the much shorter distance across the hybrid zone. It may take numerous generations for a gene to travel such a distance, and this will vary among taxa with different dispersal rates. To facilitate comparisons among taxa, we also express the barrier strength in terms of traveling time under a neutral diffusion model. Thus,

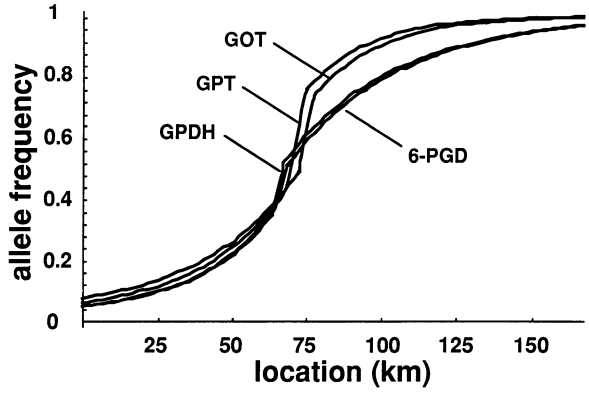

FIG. 3. Maximum-likelihood cline shapes of the four loci, estimated independently, against the *edusa* allele frequency. The clines differ mainly by the degree of introgression into *edusa*. Shape parameter estimates are given in Table 3, and are compared statistically in Table 4.

$$T_L = \left(\frac{\beta_L}{\sigma}\right)^2 \quad (11a)$$

$$T_R = \left(\frac{\beta_R}{\sigma}\right)^2 \quad (11b)$$

are the traveling times in generations required for a neutral gene to reach the opposite side of the barrier (Barton and Gale 1993). T is a useful measure of genetic isolation.

The algorithm for fitting all loci simultaneously was run for 7000 iterations during the annealing process to estimate the shape parameters S. Then another 7000 iterations were run on the best-fitting shape during annealing to find the best-fitting estimate of D. The simulation was then run until 2000 replicates within the two-unit support limits were obtained.

RESULTS

Hybrid Zone Genotypes

Populations in the hybrid zone yielded numerous individuals that showed complex hybrid ancestry based on allozyme markers. Few individuals were heterozygous at all four marker loci, and introgressed diagnostic markers appeared at low frequencies as far as 125 km from the center of the zone. We found marked deviations from Hardy-Weinberg proportions ($F_{IS} = 0.65$) for populations within 25 km of the hybrid zone center. This may be partly due to long distance movements of "pure" genotypes across the zone, and partly due to selection against recombinant genotypes. We did find examples of possible long-distance migrants of "pure" marker-allele genotypes as far as 15 km into the *daplidice* side and up to 48 km into the *edusa* side.

Single-Locus Clines

The clines at each locus are shown in Figure 3 and the parameter estimates and 2-unit support limits are given in Table 3. The positions of the clines are relatively concordant, centered within 6 km of one another and showing overlapping

TABLE 3. Cline shape parameter estimates (two-unit support limits) for each locus assessed independently.

	GOT	GPT	GPDH	6-PGD
$L(S)$	−164.924	−142.833	−185.038	−208.435
c	72.85 (65.71–73.32)	69.84 (64.10–71.63)	67.06 (66.12–72.80)	68.25 (65.73–73.02)
w	18.95 (18.37–22.12)	19.00 (18.79–22.50)	25.15 (23.15–26.67)	23.43 (20.16–25.25)
θ_L	0.020 (0.019–0.033)	0.027 (0.023–0.050)	0.061 (0.039–0.069)	0.047 (0.032–0.071)
θ_R	0.044 (0.029–0.053)	0.050 (0.040–0.068)	0.029 (0.025–0.046)	0.025 (0.020–0.032)
z_L	23.93 (23.85–24.22)	23.19 (23.12–23.53)	23.45 (22.99–23.54)	24.89 (24.80–25.11)
z_R	25.12 (24.81–25.22)	24.50 (24.39–24.69)	26.05 (25.59–26.05)	25.72 (25.35–25.76)
x_L	72.48 (63.49–73.10)	68.39 (60.98–71.00)	62.77 (61.05–70.97)	64.53 (59.99–70.71)
x_R	77.68 (68.00–78.49)	75.17 (69.42–78.53)	67.23 (66.42–74.47)	68.28 (65.74–73.58)
β_L	17.58 (9.58–25.06)	22.34 (14.78–34.62)	12.91 (4.24–23.80)	12.05 (4.46–23.46)
β_R	21.68 (10.28–32.49)	28.54 (17.19–47.00)	12.83 (4.57–22.60)	11.48 (4.54–18.78)

two-unit support limits, and located near the valley of the Scrivia River (Fig. 1). All the clines are characterized by generally similar widths, and with broad and roughly symmetrical tails of introgression on either side.

Upon closer inspection, the single-locus clines appear to fall into two groups (Fig. 3), and the significance of the differences in their shapes can be assessed using likelihood. Let S_{GOT}, S_{GPT}, S_{GPDH}, and $S_{6\text{-}PGD}$ be the best-supported set of shape parameters for each of the loci, as given in Table 3. Let $L(S_{GOT}|\text{GOT})$ be the likelihood of S_{GOT} given the data for the GOT locus, and $L(S_{GPT}|\text{GOT})$ be the likelihood of the GPT shape parameters assessed against the same GOT data. The S_{GOT} and S_{GPT} clines differ relative to the GOT data by $\Delta L = L(S_{GOT}|\text{GOT}) - L(S_{GPT}|GOT)$, and this is significant at level α if $G = 2\Delta L > \chi^2_{\text{df},\alpha}$. The degrees of freedom are df = (2 alleles − 1)(28 populations − 6 parameters estimated − 1) = 21. Table 4 gives the differences ΔL among the shapes, and their associated significance levels. The locus 6-PGD is significantly different from both GOT and GPT when assessed against the 6-PGD data, and GPDH is marginally significantly different from GPT using the GPDH data. The reciprocal comparisons, however, do not show significance, because of rather high variability among sites in the GOT and GPT allele frequencies. Unplanned followup analyses were done to assess the source of the significant differences, by considering separately the fit of these shapes to the data from the *daplidice* side (locations between 0 and the center c) and the *edusa* side (locations from c to 167). On the *edusa* side, the tests have df = (15 *edusa* populations −4 parameters estimated −1)=10, since the fit is not influenced by the θ_L and z_L estimates from the *daplidice* side of the zone. None of the ΔL comparisons were significant on the *daplidice* side ($P > 0.81$), and all previously significant comparisons retained their significance on the *edusa* side (Table 4). Thus, deviations in single-locus shapes are due almost entirely to differences in the shapes of the introgressing tails on the *edusa* side of the zone. We can explore causes of these differences with information from averages of all the loci taken together.

Inferences from Multilocus Cline Shape and Disequilibrium

Hybrid Zone Location and Shape.—The best-fit multilocus average cline is shown in Figure 4, and Table 5 gives the parameter estimates and support limits obtained. As expected, the overall patterns of shape and location differ negligibly from those of the single-locus clines (Fig. 3), which were reasonably concordant. However, the multilocus cline re-

TABLE 4. Tests for differences in shape among the single-locus clines. Shown are differences in support (ΔL_{df}) among the best-fit cline shapes (S) at different loci, assessed against the data for each locus. P-values are obtained from a χ^2 distribution using $G = 2\Delta L$. Unplanned follow-up tests on the significantly different pairs use data from the *edusa* side; no significant variation among shapes appeared on the *daplidice* side. In these tests, df = 10 since parameters θ_L and z_L do not influence the shape on the *edusa* side.

Comparison	Data from the entire transect		Unplanned follow-up tests	
	ΔL_{21}	P	ΔL_{10}	P
$L(S_{GOT} \mid \text{GOT}) - L(S_{GPT} \mid \text{GOT})$	1.32	0.999		
$L(S_{GOT} \mid \text{GOT}) - L(S_{GPDH} \mid \text{GOT})$	9.46	0.590		
$L(S_{GOT} \mid \text{GOT}) - L(S_{6\text{-}PGD} \mid \text{GOT})$	10.01	0.521		
$L(S_{GOT} \mid \text{GOT}) - L(S_{ave} \mid \text{GOT})$	0.97	0.999		
$L(S_{GPT} \mid \text{GPT}) - L(S_{GOT} \mid \text{GPT})$	1.06	0.999		
$L(S_{GPT} \mid \text{GPT}) - L(S_{GPDH} \mid \text{GPT})$	11.96	0.297		
$L(S_{GPT} \mid \text{GPT}) - L(S_{6\text{-}PGD} \mid \text{GPT})$	13.21	0.191		
$L(S_{GPT} \mid \text{GPT}) - L(S_{ave} \mid \text{GPT})$	1.60	0.999		
$L(S_{GPDH} \mid \text{GPDH}) - L(S_{GOT} \mid \text{GPDH})$	12.17	0.277		
$L(S_{GPDH} \mid \text{GPDH}) - L(S_{GPT} \mid \text{GPDH})$	16.98	0.0365	16.83	2.10×10^{-4}
$L(S_{GPDH} \mid \text{GPDH}) - L(S_{6\text{-}PGD} \mid \text{GPDH})$	0.24	1.00		
$L(S_{GPDH} \mid \text{GPDH}) - L(S_{ave} \mid \text{GPDH})$	6.15	0.931		
$L(S_{6\text{-}PGD} \mid \text{6-PGD}) - L(S_{GOT} \mid \text{6-PGD})$	25.19	3.23×10^{-4}	23.96	6.40×10^{-7}
$L(S_{6\text{-}PGD} \mid \text{6-PGD}) - L(S_{GPT} \mid \text{6-PGD})$	32.79	1.76×10^{-6}	32.41	4.40×10^{-10}
$L(S_{6\text{-}GPD} \mid \text{6-GPD}) - L(S_{GPDH} \mid \text{6-PGD})$	0.40	1.00		
$L(S_{6\text{-}PGD} \mid \text{6-PGD}) - L(S_{ave} \mid \text{6-PGD})$	15.50	0.0735		

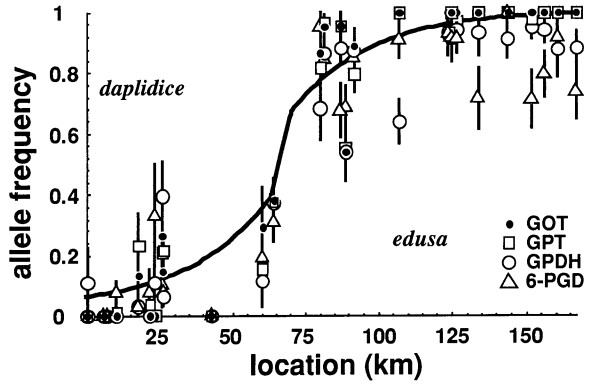

FIG. 4. Mean ± SD of the *edusa* allele frequencies for each transect location, with the line representing the best fit shape of the multilocus average cline. Shape parameter estimates are given in Table 4.

solves to be somewhat wider than any of the single-locus clines, because its width includes variation among the center locations of the single-locus clines in addition to minor variation in their widths.

Disequilibrium

The variation in cline shape yielded three sets of populations that fell into the central region, defined to be within 25 km of the center. We used maximum likelihood to estimate disequilibrium, and since the likelihood model differs depending on which populations fall in the central region, we calculated D for all three population sets. The disequilibrium was high, yielding an average of $D = 0.148$ (0.141–0.150), with the two-unit support limits taken over all central population sets. Hybrid zone models reviewed by Barton and Gale (1993) indicate that much of this disequilibrium is maintained by selection on loci in the central region of the zone, following dispersal into this region.

Dispersal

When estimated (eq. 6) from the relationship between disequilibrium and multilocus cline width, dispersal is fairly high, on the order of $\sigma = 6.3$ (5.8–6.7) km/gen$^{1/2}$ (Table 7). This may be too high, however, since the multilocus cline width is broadened by variation among center locations, and equation(6) assumes concordance among single-locus clines. When disequilibrium estimates are used in equation(6) with the single-locus cline widths, dispersal resolves to $\sigma = 4.5$ (3.7–5.5) km/gen$^{1/2}$ (Tables 6 and 7), a significantly lower estimate. The value given here is the average of maximum-likelihood estimates of each of the four loci (Table 6), and the support limits are the extreme values over all four loci.

TABLE 5. Cline shape parameter estimates (two-unit support limbs) based on shape and disequilibrium. For the average cline, tabled values of D and the parameters below it are averages of maximum-likelihood estimates taken over three different sets of central populations yielded by variation in cline shape, and the support limits are taken from extremes over these population sets combined.

	Average cline
$L(S)$	−649.816
c	67.56 (65.92–70.76)
w	28.19 (26.14–29.47)
θ_L	0.065 (0.054–0.078)
θ_R	0.070 (0.059–0.080)
z_L	23.12 (22.72–23.21)
z_R	25.65 (25.40–25.76)
x_L	64.25 (61.72–68.08)
x_R	73.19 (70.26–77.23)
D	0.148 (0.139–0.153)
β_L	21.9 (16.4–28.5)
β_R	26.3 (19.6–34.4)

Effective Selection

Selection appears to be strong against hybrids in the center of the zone. The single-locus model (eq. 1b) fit to the central region represents the same shape that would be produced as if only one locus was responsible for the entire cline shape. The effective strength of selection, s^* needed to produce this central-region cline in the face of dispersal is obtained from the relationship between dispersal and cline width (eq. 6), and this also depends on the type of selection. Such selection may be "intrinsic," s^*_{in}, caused by maladaptive epistatic interactions among loci, or "extrinsic," s^*_{ex}, caused by inappropriate genetic responses to environmental conditions.

Table 7 shows selection estimated from the multilocus cline width when the corrected dispersal value of $\sigma = 4.5$ is used. If the cline is entirely produced by epistatic interactions, then effective selection is quite strong at $s^*_{in} = 0.560$ (0.508–0.639). If the cline is entirely caused by adaptation to local environments, which seems unlikely given the apparent uniformity of habitat, then the effective strength of selection is only slightly lower at $s^*_{ex} = 0.521$ (0.472–0.595). In natural situations, most clines are probably produced by contributions from each of these sources, and a reasonably strong statement about the overall strength needed can be obtained by combining the support limits, yielding $0.472 \leq s^* \leq 0.639$. If multilocus cline width is used for the dispersal estimate,

TABLE 6. Derived parameter estimates for the single-locus clines, incorporating the disequilibrium estimate from the average cline.

	GOT	GPT	GPDH	6-PGD
σ	4.18 (3.68–4.47)	4.03 (3.80–4.62)	5.05 (4.60–5.48)	4.64 (4.09–5.20)
s^*_{in}	0.639 (0.627–0.642)	0.638 (0.627–0.642)	0.638 (0.627–0.642)	0.638 (0.627–0.642)
s^*_{ex}	0.595 (0.583–0.597)	0.594 (0.583–0.597)	0.594 (0.583–0.597)	0.594 (0.583–0.597)
s_{eL}	0.0169 (0.0123–0.0214)	0.0206 (0.0148–0.0319)	0.0363 (0.0244–0.0443)	0.0294 (0.0205–0.0457)
s_{eR}	0.0287 (0.0181–0.0340)	0.0335 (0.0250–0.0433)	0.0194 (0.0157–0.0293)	0.0152 (0.0128–0.0203)
T_L	17.8 (5.1–42.8)	37.1 (10.9–77.0)	6.1 (0.7–23.7)	7.7 (0.9–23.2)
T_R	25.0 (6.1–71.9)	56.8 (15.1–131)	6.4 (0.8–21.4)	6.8 (0.9–18.1)

TABLE 7. Derived parameter estimates for the average cline, incorporating the dispersal estimate derived from the multilocus cline width, and again using the average of the dispersal estimates derived from the single-locus cline widths (Table 6). The second column is included for comparison to other studies, but is probably biased because the multilocus cline width is an average over slightly different center positions of the single-locus clines.

	σ from average of single-locus clines		σ from multilocus cline	
σ	4.41	(3.68–5.48)	6.30	(5.79–6.65)
s^*_{in}	0.560	(0.508–0.639)	0.201	(0.185–0.204)
s^*_{ex}	0.521	(0.472–0.595)	0.151	(0.139–0.153)
s_{eL}	0.0376	(0.0295–0.0472)	0.0132	(0.0106–0.0157)
s_{eR}	0.0367	(0.0309–0.0492)	0.0135	(0.0117–0.0163)
T_L	25.5	(10.1–49.7)	12.1	(6.6–21.0)
T_R	34.1	(14.5–74.1)	16.7	(9.1–30.3)

such that σ = 6.3, then estimated effective selection resolves to the range of $0.139 \leq s^* \leq 0.204$ (Table 7), markedly lower but still strong. This effective selection strength is consistent with the moderate frequency of recombinant genotypes and the strong deviations from Hardy-Weinberg proportions observed in the zone. This selection, while strong, is not enough to provide anything like a complete barrier to gene flow.

Barrier Strength and Differential Introgression into "Pure" Populations

Barrier strength may be considered as (1) β, the distance along a smooth cline that a gene would have to travel to make up the frequency difference seen in the central step between equations (1a) and (1c); or (2) *T*, the time in generations it would take a gene to travel this distance by neutral diffusion across the zone. This barrier strength is measured from cline shape in the first case, and from cline shape and estimated dispersal in the second case. These values may differ on either side of the zone, depending on the local strengths of selection, and they may also vary among marker loci.

The shape of the multilocus cline shows broad tails of introgression with only negligible asymmetry (Fig. 4, Table 5). On the *daplidice* side, the point x_L is only 3 km away from the center, and x_R on the *edusa* side is only 4 km away, such that foreign alleles occur at high frequencies in populations near the center of the zone. θ, which describes the decay in frequency in the tails of the zone relative to the shape of the central portion, is significantly less than one in both tails, indicating that the introgressing marker alleles experience relatively shallow declines in frequency away from the much steeper center of the zone.

The shallowness of clines near the center of the zone produces a minor barrier to introgression of an average neutral allele crossing the zone. The multilocus cline provides a barrier equivalent to isolation by distance of only $\beta_L = 21.9$ (16.4—28.5) km for genes crossing from *daplidice* into *edusa*, and a possibly slightly higher barrier of $\beta_R = 26.3$ (19.6–34.4) km for genes traveling in the opposite direction (Table 5). Given the high vagility of these butterflies (Table 7), such distances may be crossed by neutral diffusion in relatively few generations: $T_L = 25.5$ (10.1–49.7) generations from *daplidice* to *edusa*, and $T_R = 34.1$ (14.5–74.1) generations from *edusa* to *daplidice*. With two to three generations annually, an average gene will cross the barrier in either direction within roughly five to 40 years. If the higher dispersal estimate from the multilocus cline is used, then these barriers drop by roughly half (Table 7).

The shapes of the single-locus clines differ significantly on the *edusa* side of the zone (Table 3), and this difference suggests that we might find variation in barrier strengths among loci (Table 3). Such a phenomenon would be expected in principle from variation in disequilibria among marker loci and loci directly responsible for the cline shape. The support limits on these estimates are relatively wide and overlap broadly, so there is not enough information available in the data to make firm conclusions, but the trends nevertheless point in the expected directions. GOT and GPT have individual barrier strengths on the order of about 20 km, which would take about 20-50 generations to cross (Table 6), whereas GPDH and 6-PGD have barrier strengths on the order of about 12 km (Table 3), which would take about six to eight generations to cross (Table 6). As in the case of the multilocus cline, none of these is a particularly strong barrier.

Selection on Introgressing Marker Alleles

From the multilocus cline, the strength of selection acting directly on an average marker locus is symmetrical in the introgressing tails of the zone, with $s_e \approx 3.7\%$. This seems rather high for allozymes, and we suspect that our estimate includes some effects of hitchhiking with selected loci that are physically linked to these allozyme markers. The tails of the hybrid zone join quite near to the central region, and close linkages probably do not have sufficient time to decay to zero near these junctions, as the model formally assumes.

We can also investigate the strengths of selection acting on each of the marker loci taken separately, by interpreting the single-locus cline shapes using the dispersal estimate obtained from disequilibrium analysis. Results of this analysis are shown in Table 6. This is most interesting on the *edusa* side of the zone, where the clines differ in their shapes. We find that selection on individual loci on the *edusa* side is somewhat stronger for GOT and GPT ($s_{eR} \approx 2.9$–3.3%) than it is for GPDH and 6-PGD ($s_{eR} \approx 1.5$–2.0%). This pattern appears to reverse itself on the *daplidice* side, where selection appears strongest against GPDH and 6-PGD. As for the multilocus cline, these coefficients probably include selection on loci closely linked to these allozyme markers. Taken together, these results imply that selection varies in intensity among markers, and it also differs in strength on either side of the hybrid zone.

We do not report $\bar{W}_h/\bar{W}_p$, the mean fitness deficit of hybrids, as did Szymura and Barton (1986, 1991; Barton and Gale 1993; Szymura 1993), because this estimate depends on an assumption that loci under selection are rather evenly distributed throughout the genome (Barton 1983; Barton and Gale 1993). While this seems valid for *Bombina* (Szymura and Barton 1986, 1991), given the numerous morphological and life-history differences seen there (Sanderson et al. 1992; Szymura 1993; Nürnberger et al. 1995), the assumption seems too tenuous invoke for the *Pontia* zone. One may also estimate the effective number of loci under selection, which resolves to $n_e = 0.39$ (0.34–0.45) for the *Pontia* zone. This

is clearly too low, and since it too depends on the assumption of an even distribution of weakly selected loci across the genome, we can only come away with a loose qualitative interpretation: The effective number of loci under selection in the *Pontia* zone is probably fairly low.

Discussion

Gene Flow and Selection in the Cline

The *P. daplidice-edusa* hybrid zone is characterized by strong selection ($s^* = 0.56$; Table 7) that enforces a steep central region, and high dispersal ($\sigma = 4.5$ km/gen$^{1/2}$; Table 7) that spreads tails of introgressing alleles over a wide area around the zone. The introgression tails join quite closely to the central portion of the best-supported cline (Figs. 3, 4), leaving a narrow central region that is roughly half the diameter of a single genetic neighborhood. This selection strength is higher than has been reported for other hybrid zones ($s^* \approx 0.23$ for *Heliconius* butterflies [Mallet et al. 1990]; $s^* = 0.17$ for *Bombina* toads [Szymura and Barton 1991]). The high value of s^* is stronger than the weak selection that is assumed in the derivation of equation (1b). Mallet et al. (1990) give simulation results that indicate that such estimates should not be unduly biased up to their highest-tested selection strengths of $s \approx 0.25$ in clines generated by frequency-dependent selection, which yields similar patterns to other types of selection (Barton and Gale 1993). Given that the central region is tightly constrained by the broad tails of introgression, and is only about one-half of a genetic neighborhood in width, we believe that any estimation biases are likely to be negligible relative to sampling error.

Patterns of cline shape in marker loci of the *Pontia* hybrid zone (Figs. 3, 4) may be seen under three sets of circumstances, which we cannot formally distinguish. They may be produced by strong selection on a small number of loci or linkage groups, which themselves maintain a steep cline, but which permit recombining marker alleles to form shallow clines on either side of the zone. The clines in the actual loci responsible for the barrier might be steep and narrow throughout, without appreciable introgressing tails as seen in the markers, which themselves may recombine away from the strongly selected loci. This is the simplest explanation, which we favor. A second possibility is that the steepness of the central portion might be explained by epistatic interactions among several loci or linkage groups. Barton and Gale (1993) give a useful descriptive model relating the fitness effect of such epistatic interactions to cline shape. Using $\bar{p}$ as the mean *edusa* allele frequency, fitness under epistasis may be described as $W(\bar{p}) = 1 - s\,[4\,\bar{p}\,(1 - \bar{p})]^{\gamma}$. When $\gamma \gg 1$, only individuals with nearly F_1 hybrid genotypes suffer reduced fitness. The multilocus shape of the *Pontia* cline (Fig. 4) corresponds well to the cases of strong epistasis among several loci, in the range of $\gamma = 4$–16 (their fig. 2-2c). In this case, the loci directly responsible for cline shape would have quite similar cline shapes to those of the marker loci. However, it becomes difficult to envision a physiological mechanism that would produce such a high γ with numerous loci, so we do not favor this explanation. A third mechanism for a steep and narrow central portion of a hybrid zone occurs when a physical barrier inhibits dispersal, as is seen across a narrow stream in the flightless grasshopper *Podisma pedestris* at Col de la Lombarde in France (Barton and Gale 1993, fig. 2-8). We do not believe the Strezia River to be capable of producing such a barrier, given the high dispersal rate in *Pontia* and its propensity for colonizing new sites, and the lack of evidence for additional barriers across nearby rivers of similar size.

We did find evidence of relatively high selection against the allozyme markers (s_{eL} and $s_{eR} > 1.5\%$) in the tails of the hybrid zone (Table 6), though this is considerably weaker than the effective selection acting in the middle of the zone. We do not believe that these values are due entirely, as the model suggests, to direct selection on the allozymes themselves. The tails join very closely to the central region of the cline, and disequilibria between markers and any closely linked selected loci probably would not have fully broken up so near to the center. These disequilibria would act to increase somewhat the slopes of the tails (θ), increasing the selection estimates there. We therefore believe that s_{eL} and s_{eR} mainly represent selection on closely linked loci, with only minor contributions from selection on the markers themselves.

Dispersal

The dispersal estimate σ and all parameters derived from it are sensitive to variation in the width of the hybrid zone. In the multilocus average cline, the average width includes variation in the center locations of the single-locus clines, and using this multilocus width significantly increases our dispersal estimate (Table 7) and sharply reduces the selection estimates, relative to the estimates based on the mean of independently estimated single-locus cline widths. We prefer the lower of the two dispersal rates in Table 7, where the bias is removed. The dispersal estimate is also sensitive to variation in the disequilibrium estimate. We took this variation into account in our estimation procedures, so the confidence limits of all values dependent upon dispersal reflect this source of error.

Our calculated dispersal rate of $\sigma = 4.5$ (3.7–5.5) km/gen$^{1/2}$ (Table 7) might seem high for such a small organism, but it agrees with previous observations of high dispersal in these and related species. These butterflies appear to rapidly colonize their early successional habitats, being found readily on small patches of suitable habitat (Courtney and Chew 1987), and they appear as strays at locations well beyond the boundaries of their normal breeding ranges (e.g., Ebert 1991). Other pierid butterflies with similar life histories are readily recaptured at distances greater than 1 km (Baker 1968; Jones et al. 1980; Chew 1981; our unpubl. data), and even these studies may have underestimated distances somewhat because of limited sampling regions, and because there may be temporal variation in dispersal associated with local phenological changes in habitat quality. Even butterflies that have been considered relatively sedentary have dispersal rates that have turned out to be fairly high. The territorial butterfly *Heliconius erato* shows a dispersal rate of $\sigma = 2.6$ km/gen$^{1/2}$ when estimated from hybrid zone shape, and the dispersal rate of its congener, *H. melpomone*, resolves to $\sigma = 3.7$ km/gen$^{1/2}$ (Mallet et al. 1990), and there is evidence

that these disperse soon after emergence before settling into territories. Mallet (1993) points out that the high genetic similarity among *Heliconius* populations also implies relatively high dispersal rates.

Differential Introgression for Marker Loci

We found differences in the shapes of the single-locus clines (Fig. 3), and these were significantly different in the extreme cases (Table 4). 6-PGD is sex-linked and differs most (Table 4) from the others, which are autosomal. Their linkages are unknown, but with 26 autosomes of roughly equal size, the chances are negligible ($P = 3/25^2 = 0.005$) that any two autosomal markers are linked. All loci experience the same dispersal rates, so the differences in cline shape can only be due to differences in selection correlated with each marker. These correlations may arise via chance, linkage, epistasis, or correlated selection on independently evolving traits (Armbruster and Schwaegerle 1996). For these allozyme markers, usually presumed to be nearly neutral, we assume selection and epistasis are negligible, leaving only linkage effects in the cases where significant differences were found. We expect that each marker locus will ultimately prove to be linked to one or more different weakly selected traits, each experiencing different selection intensities. This seems the most likely explanation for the differences seen among s_{eL} and s_{eR} for the different marker loci (Table 6).

Historical Inferences

The shape of the *Pontia* hybrid zone, as described from allozyme markers, suggests a system that has differentiated in allopatry and come into secondary contact. If the system had evolved by primary contact, then one would have to explain how the allozymes, probably nearly neutral themselves, would have such similar patterns of geographic differentiation. This would require strong, geographically correlated selection directly on each of the allozyme markers, and we can imagine no reasonable scenario for independent selection on so many allozymes concordantly. More plausible is allopatric differentiation, followed by secondary contact in the Quaternary (Pleistocene or Holocene). Any specific scenario would have to be highly speculative. Kostrowicki (1969) classified *daplidice* (including *edusa*) as a "transpalearctic (continuous) element" of "meridional-transcontinental distribution," reflecting its preference for dry, warm-summer climates seemingly including both mild-winter (Mediterranean) and very cold-winter (steppe) habitats. He suggested that such species had originated in central Asia and spread westward in two waves, one Tertiary (including *daplidice*) and the other in the early to mid-Pleistocene. Since Kostrowicki wrote, the picture of Quaternary vegetational dynamics has changed considerably. Huntley and Birks (1983) and Peterson (1983a,b), based on numerous pollen floras, supplanted Frenzel's (1968) paleovegetational reconstruction, and Huntley (1988) provided multivariate reconstructions of European paleovegetational associations through time. Overall, the picture presented is complex (Tallis 1991; Lang 1994), but it is evident that summer aridity is of recent origin in the Mediterranean basin and has progressed there from east to west. Between 6000 and 12,000 years ago, summer precipitation seems to have been much more widespread and abundant in the region, and the flora was more typical of that in northern Europe, where *daplidice* does not occur. Much of the present Mediterranean flora was confined to the southern third of the Saharan region, and the dry, steppe habitats now occupied by *P. daplidice* (sens. lat.) in central Asia were widespread from eastern Europe through central India. Modern climatic regimes (and vegetations) became established only 4000–6000 years ago, and the usual weedy habitats occupied by *Pontia* in the Mediterranean basin today were probably not widespread before the advent of agriculture (Tallis 1991). This suggests a scenario, among many others, with *daplidice* in Africa and *edusa* in the middle East and south-central Asia on the steppe at the onset of the Holocene. What is clear from paleovegetational reconstructions is that we must consider possible geographic range changes of *daplidice*-group taxa in the past several thousand years over a very broad scale, extending at least to central Africa and west-central Asia.

Genetic Isolation and "Diagnostic" Alleles

In spite of the consistent allozyme differences and minor morphological differences between these taxa (Geiger et al. 1988), there is ample opportunity for neutral gene exchange across their hybrid zone. The barrier to introgression of marker loci is weak, being $T = 56$ generations or less, and at most only 131 generations (Table 6). This means that populations on two sides of the hybrid zone have the same proportion of identical-by-descent neutral alleles as do populations separated by distances of less than $\beta = 25$ km within either of the "pure" species ranges.

Why hasn't the system become homogenized if there is so much gene flow? Such a process would be expected to take a very long time after secondary contact (Endler 1977). After crossing the barrier, neutral alleles increase in frequency mainly by drift, and are spread by gene flow. It is difficult for a migrating allele to enter an established population as an immigrant, as it might well be lost by drift within the first few generations. Biasing this drift in favor of increase is the weakened migration pressure of genes that filter through the barrier (Barton 1983; Barton and Bengtsson 1986), but this pressure becomes negligible after a few dispersal distances from the edge of the zone, where it countered by native alleles dispersing into the region. Additionally, many hybrid zones are centered in areas of low population density, whereby an allele must also win an uphill fight against migration pressure from the high end of a density gradient to increase in frequency. Thus, the farther into the geographic range, the less likely one is to find copies of the foreign allele. This is a basic problem for the spread of any nearly neutral allele in an isolation-by-distance context, not only across hybrid zones. We shouldn't necessarily expect gene flow to rapidly homogenize any system at large spatial scales.

Relating the Biology to the Systematics

These butterfly populations are probably best thought of as well-differentiated subspecies. Neutral alleles are crossing the boundary at their contact areas, and are slowed only by weak barriers to introgression and by the standard, isolation-

by-distance problems that always limit the spread of new neutral alleles across continuous populations. The allozyme frequencies have not become homogenized over the entire geographic ranges probably because this takes such a very long time to accomplish, although foreign alleles do appear to have spread over 100 km into the established ranges of the two taxa. However, adaptive alleles will easily spread, as the hybrid zone will create only a momentary barrier, with selection pulling them across once they appear on the opposite side (Barton and Bengtsson 1986). We wouldn't say that separate *P. daplidice* populations in, say, France and Morocco were genetically isolated, but in fact, such distant populations may be more isolated genetically than are *daplidice* and *edusa* populations on opposite sides of their hybrid zone near Genoa. Despite the differences they display, the evolutionary histories of the genomes of *P. daplidice* and *P. edusa* appear to be inextricably linked in the long term.

Acknowledgments

The analyses were supported by grant #31-32463.91 from the Swiss National Science Foundation. Additional support was obtained from the Dr. K. Bretscher Stiftung (University of Berne), an Academic Challenge grant to the Biological Sciences Department at BGSU, and BGSU Faculty Research Committee grants to AHP. L. Frauchiger and V. Siegfried provided their typically excellent technical assistance during the electrophoresis. We thank Bob Hagen for helpful discussion.

Literature Cited

Armbruster, W. S., and K. E. Schwaegerle. 1996. Causes of covariation of phenotypic traits among populations. J. Evol. Biol. 9:261–276.

Baird, S. J. E. 1995. A simulation study of multilocus clines. Evolution 49:1038–1045.

Baker, R. R. 1968. Sun orientation during migration in some British butterflies. Proc. R. Ent. Soc. Lond. (A) 43:89–95.

Barton, N. H. 1979. Gene flow past a cline. Heredity 43:333–339.

———. 1983. Multilocus clines. Evolution 37:454–471.

Barton, N. H., and B. O. Bengtsson. 1986. The barrier to genetic exchange between hybridising populations. Heredity 56:357–376.

Barton, N. H., and K. S. Gale. 1993. Genetic analysis of hybrid zones. Pp. 13–45 *in* R. G. Harrison, ed. Hybrid zones and the evolutionary process. Oxford Univ. Press, Oxford.

Barton, N. H., and G. M. Hewitt. 1983. Hybrid zones as barriers to gene flow. Pp. 341–359 *in* G. S. Oxford and D. Robinson, eds. Protein polymorphism: adaptive and taxonomic significance. Academic Press, New York.

———. 1985. Analysis of hybrid zones. Ann. Rev. Ecol. Syst. 16: 113–148.

Buchi, L. 1996. Untersuchung von Mechanismen der reproduktiven Isolation der Resedafalter *Pontia daplidice* und *Pontia edusa* (Lepidoptera: Pieridae). Diploma (master's) thesis, Univ. of Berne, Berne, Switzerland.

Chew, F. S. 1981. Coexistence and local extinction in two pierid butterflies. Am. Nat. 118:655–672.

Cockerham, C. C., and B. S. Weir. 1993. Estimation of gene flow from *F*-statistics. Evolution 47:855–863.

Courtney, S. P., and F. S. Chew. 1987. Coexistence and host use by a large community of pierid butterflies: habitat is the templet. Oecologia 71:210–220.

Coyne, J. A., H. A. Orr, and D. J. Futuyma. 1988. Do we need a new species concept? Syst. Zool. 37:190–200.

Crow, J. F., and K. Aoki. 1984. Group selection for a polygenic behavioral trait: estimating the degree of population subdivision. Proc. Nat. Acad. Sci. USA 81:6073–6077.

Ebert, G. 1991. Die Schmetterlinge Baden-Württembergs, Band 1. Eugen Ulmer GmbH & Co., Stuttgart.

Edwards, A. 1992. Likelihood. Johns Hopkins Univ. Press, Baltimore, MD.

Endler, J. A. 1977. Geographic variation, speciation, and clines. Princeton Univ. Press, Princeton, NJ.

Frenzel, B. 1968. Grundzüge der pleistozänen Vegetationsgeschichte nordeurasiens. F. Steiner Verlag, Wiesbaden.

Geiger, H. J. 1981. Enzyme electrophoretic studies on the genetic relationships of pierid butterflies (Lepidoptera, Pieridae). I. European taxa. J. Res. Lep. 19:181–195.

Geiger, H. J., and A. Scholl. 1985. Systematics and evolution of holarctic Pierinae (Lepidoptera). An enzyme electrophoretic approach. Experientia 41:24–29.

Geiger, H. J., H. Descimon, and A. Scholl. 1988. Evidence for speciation within nominal *Pontia daplidice* (Linnaeus, 1758) in southern Europe (Lepidoptera, Pieridae). Nota lepid. 11:7–20.

Harrison, R. G., ed. 1993. Hybrid zones and the evolutionary process. Oxford Univ. Press, Oxford.

Hill, W. G. 1974. Estimation of linkage disequilibrium in randomly mating populations. Heredity 33:229–239.

Huntley, B. 1988. Europe. Pp. 341–383 *in* B. Huntley and T. Webb, III, eds. Vegetation history. Kluwer Academic, Dordrecht.

Huntley, B., and H. J. B. Birks. 1983. An atlas of past and present pollen maps for Europe. Cambridge Univ. Press, Cambridge.

Jones, R. E., N. Gilbert, M. Guppy, and V. Nealis. 1980. Long-distance movement of *Pieris rapae*. J. Anim. Ecol. 49:629–642.

Kostrowicki, A. S. 1969. Geography of the Palearctic Papilionoidea. Panstwowe Wydawnictwo Naukowe, Krakow.

Lang, G. 1994. Quartäre Vegetationsgeschichte Europas: Methoden und Ergebnisse. Jena, Stuttgart.

Mallet, J. 1993. Speciation, raciation, and color pattern evolution in *Heliconius* butterflies: Evidence from hybrid zones. Pp. 226–260 *in* R. G. Harrison, ed. Hybrid zones and the evolutionary process. Oxford Univ. Press, Oxford.

Mallet, J., N. H. Barton, G. Lamas, J. Santisteban, M. Muedas, and H. Eeley. 1990. Estimates of selection and gene flow from measures of cline width and linkage disequilibrium in *Heliconius* hybrid zones. Genetics 124:921–936.

Nürnberger, B., N. H. Barton, C. MacCallum, J. Gilchrist, and M. Appleby. 1995. Natural selection on quantitative traits in the *Bombina* hybrid zone. Evolution 49:1224–1238.

Otte, D., and J. A. Endler. 1989. Speciation and its consequences. Sinauer, Sunderland, MA.

Peterson, C. 1983a. Holocene vegetation and climate in the western USSR. Ph.D. diss. Univ. of Wisconsin, Madison.

———. 1983b. Recent pollen spectra and zonal vegetation in the western USSR. Quatern. Sci. Rev. 2:281–321.

Porter, A. H. 1990. Testing nominal species boundaries using *F*-statistics: the taxonomy of two hybridizing admiral butterflies (*Limenitis*: Nymphalidae). Syst. Zool. 39:131–148.

Porter, A. H., and H. J. Geiger. 1988. Genetic and phenotypic population structure of the *Coenonympha tullia* complex (Lepidoptera: Nymphalidae: Satyrinae) in California: no evidence for species boundaries. Can. J. Zool. 66:2751–2765.

———. 1995. Limitations to the inference of gene flow at regional geographic scales—an example from the *Pieris napi* group (Lepidoptera: Pieridae) in Europe. Biol. J. Linn. Soc. 54:329–348.

Press, W. H., B. P. Flannery, S. A. Teukolsky, & W. T. Vetterling. 1989. Numerical recipes in Pascal. Cambridge Univ. Press, Cambridge.

Sanderson, N., J. M. Szymura, and N. H. Barton. 1992. Variation in mating call across the hybrid zone between the firebellied toads *Bombina bombina* and *B. variegata*. Evolution 46: 595–607.

Slatkin, M. 1973. Gene flow and selection in a cline. Genetics 75:733–756.

———. 1987. Gene flow and geographic structure of natural populations. Science 236:787–792.

———. 1993. Isolation by distance in equilibrium and non-equilibrium populations. Evolution 47:264–279.
SOKAL, R. R., AND N. L. ODEN. 1978. Spatial autocorrelation in biology. I. Methodology. Biol. J. Linn. Soc. 10:199–228.
SOKAL, R. R., AND F. J. ROHLF. 1995. Biometry. 3d ed. Freeman, New York.
SZYMURA, J. M. 1993. Analysis of hybrid zones with *Bombina*. Pp. 261–289 *in* R. G. Harrison, ed. Hybrid zones and the evolutionary process. Oxford Univ. Press, Oxford.
SZYMURA, J. M., AND N. H. BARTON. 1986. Genetic analysis of a hybrid zone between the fire-bellied toads, *Bombina bombina* and *Bombina variegata*, near Cracow in southern Poland. Evolution 40:1141–1159.
———. 1991. The genetic structure of the hybrid zone between the fire-bellied toads *Bombina bombina* and *B. variegata*: comparisons between transects and between loci. Evolution 45:237–261.
TALLIS, J. H. 1991. Plant community history: long-term changes in plant distribution and diversity. Chapman-Hall, London.
WAGENER, P. S. 1988. What are the valid names for the two genetically different taxa currently included within *Pontia daplidice* (Linnaeus, 1758) (Lepidoptera: Pieridae)? Nota lepid. 11: 21–38.
WEIR, B. S., AND C. C. COCKERHAM. 1979. Estimation of linkage disequilibrium in randomly mating populations. Heredity 42: 105–111.
———. 1984. Estimating *F*-statistics for the analysis of population structure. Evolution 38:1358–1370.
WENGER, R. 1993. Enzymelektrophoretisch-genetische Analyse einer Hybridzone zwischen *Pontia daplidice* (Linnaeus 1758) und *Pontia edusa* (Fabricius 1777) (Lepidoptera: Pieridae). Diploma (master's) thesis. Univ. of Berne, Berne, Switzerland.
WOLFRAM, S. 1991. Mathematica: a system of doing mathematics by computer. 2d ed. Addison-Wesley, Redwood City, CA.
WRIGHT, S. 1943. Isolation by distance. Genetics 43:114–138.

Corresponding Editor: T. Hilbish

APPENDIX

Hill (1974) provides the likelihood function for estimating gametic disequilibrium between a pair of autosomal loci, and we extend it here to include the possibility of sex-linkage for either or both loci. It is convenient to have a general function of this type when designing algorithms to estimate disequilibria. This method assumes that the between-individual component of disequilibrium (Weir and Cockerham 1979) is zero.

Consider a locus with alleles A and a, having frequencies p_A and p_a, and a second locus having alleles B and b at frequencies p_B and p_b. Either locus may be autosomal or sex-linked. $\mathbf{N}$ is a matrix of observed genotype frequencies shown in Table A1. In particular cases, many of the N_{ij} will be zero, depending on the inheritance of the loci and the sampling scheme, and these terms will drop out of the likelihood equation. The expected gamete frequencies are defined in relation to gametic disequilibrium (D) in Table A2, and the expected genotypic frequencies are given in Table A3.

TABLE A1. $\mathbf{N}$ is the matrix of potentially observable genotypic frequencies when either locus may be sex linked.

		Homogametic sex or autosome			Heterogametic sex		
		BB	*Bb*	*bb*	*B*	*b*	Totals
Homogametic sex or autosome	*AA*	N_{11}	N_{12}	N_{13}	N_{14}	N_{15}	$N_{1\cdot}$
	Aa	N_{21}	N_{22}	N_{23}	N_{24}	N_{25}	N_{2}
	aa	N_{31}	N_{32}	N_{33}	N_{34}	N_{35}	$N_{3\cdot}$
Heterogametic sex	*A*	N_{41}	N_{42}	N_{43}	N_{44}	N_{45}	$N_{4\cdot}$
	a	N_{51}	N_{52}	N_{53}	N_{54}	N_{55}	N_{5}
	Totals	$N_{\cdot 1}$	$N_{\cdot 2}$	$N_{\cdot 3}$	$N_{\cdot 4}$	$N_{\cdot 5}$	N

TABLE A2. Expected gametic frequencies when one or both loci may be sex linked, in relation to gametic disequilibrium (D).

	Gamete	Expected frequency	Expected frequency in relation to D
Homogametic sex or autosome	*A/B*	f_{11}	$p_A p_B + D$
	A/b	f_{12}	$p_A p_b - D$
	a/B	f_{21}	$p_a p_B - D$
	a/b	f_{22}	$p_a p_b + D$
Heterogametic sex, only *B* sex linked	*A/−*	$f_{1} = f_{11} + f_{12}$	p_A
	a/−	$f_{2} = f_{21} + f_{22}$	p_a
Heterogametic sex, only *A* sex linked	*−/B*	$f_{\cdot 1} = f_{11} + f_{21}$	p_B
	−/b	$f_{\cdot 2} = f_{12} + f_{22}$	p_b

The log-likelihood of D is proportional to the sum of all corresponding *observed* ln(*expected*) genotypic frequencies in Tables A1, A3,

$$\ln L(D \mid \mathbf{N}) = N_{11}\ln(f_{11}^2) + \ldots + N_{55}\ln(f_{12}) + C \qquad \text{(A1)}$$

(Hill 1974), where C is a constant of proportionality common to all likelihood functions (Edwards 1972). This sum may be expanded and rearranged such that values of N_{ij} ln(2) and N_{ij} ln($f_{i\cdot}$) = N_{ij} ln(p_A), etc., which are constant for a given dataset $\mathbf{N}$, are absorbed into C. This leaves a version in the form of Hill's (1974) likelihood function,

$$\ln L(D \mid \mathbf{N}) = \sum_{i,j}^{2} X_{ij} \ln f(D)_{ij} + N_{22}\ln[f(D)_{11}f(D)_{22} + f(D)_{12}f(D)_{21}] + C, \qquad \text{(A2)}$$

where $f(D)_{11} = f_{11} = D + p_A p_B$, etc., and $\mathbf{X}$ is a matrix of values derived from $\mathbf{N}$,

$$X_{11} = 2N_{11} + N_{12} + N_{14} + N_{21} + N_{41} + N_{44},$$
$$X_{12} = N_{12} + 2N_{13} + N_{15} + N_{23} + N_{43} + N_{45},$$
$$X_{21} = N_{21} + 2N_{31} + N_{32} + N_{34} + N_{51} + N_{54},$$
$$X_{22} = N_{23} + N_{32} + 2N_{33} + N_{35} + N_{53} + N_{55}.$$

When both loci are autosomal, or when all sampled individuals are of the homogametic sex, then this method reduces to the form given in Hill (1974). When one or both loci are sex-linked, or a haplodiploid sex determination system applies, then this method readily permits the use of data from both males and females in estimating the degree of disequilibrium. The maximum-likelihood estimate of D may then be obtained using the method proposed by Weir and Cockerham (1979), or as we have done in the accompanying paper, by using a Metropolis algorithm (Press et al. 1989).

TABLE A3. Expected genotypic frequencies when one or both loci may be sex linked.

	Autosome	Homogametic sex or autosome			Heterogametic sex	
		BB	*Bb*	*bb*	*B−*	*b−*
Homogametic sex or autosome	*AA*	f_{11}^2	$2f_{11}f_{12}$	f_{12}^2	$f_{11}f_{1\cdot}$	$f_{12}f_{1\cdot}$
	Aa	$2f_{11}f_{21}$	$2f_{11}f_{22}+$ $2f_{12}f_{21}$	$2f_{12}$ f_{22}	$f_{1\cdot}$	$f_{\cdot 2}$
	aa	f_{21}^2	$2f_{21}f_{22}$	f_{22}^2	$f_{21}f_{2\cdot}$	$f_{22}f_{2\cdot}$
Heterogametic sex	*A−*	$f_{11}f_{1}$	$f_{1\cdot}$	$f_{12}f_{\cdot 2}$	f_{11}	f_{12}
	a−	$f_{21}f_{1}$	f_{2}	$f_{22}f_{2}$	f_{21}	f_{22}